Journal of
Computational and Theoretical Nanoscience
Vol. 11, 272–282, 2014

RESEARCH ARTICLE

Artificial Neural Network Modeling and Simulation of *In-Vitro* Nanoparticle-Cell Interactions

Neslihan Cenk[1], Gurer Budak[3,*], Savas Dayanik[1], and Ihsan Sabuncuoglu[2]

[1] *Industrial Engineering Department, Bilkent University, Ankara, 06800, Turkey*
[2] *Abdullah Gul University, Kayseri, 38039, Turkey*
[3] *Nanomedicine and Advanced Technology Research Center, 06830, Turkey*

In this research a prediction model for the cellular uptake efficiency of nanoparticles (NPs), which is the rate that NPs adhere to a cell surface or enter a cell, is investigated via an artificial neural network (ANN) method. An appropriate mathematical model for the prediction of the cellular uptake rate of NPs will significantly reduce the number of time-consuming experiments to determine which of the thousands of possible variables have an impact on NP uptake rate. Moreover, this study constitutes a basis for targeted drug delivery and cell-level detection, treatment and diagnosis of existing pathologies through simulating NP-cell interactions. Accordingly, this study will accelerate nanomedicine research. Our research focuses on building a proper ANN model based on a multilayered feed-forward back-propagation algorithm that depends on NP type, size, surface charge, concentration and time for prediction of cellular uptake efficiency. The NP types for *in-vitro* NP-healthy cell interaction analysis are polymethyl methacrylate (PMMA), silica and polylactic acid (PLA), all of whose shapes are spheres. The proposed ANN model has been developed on MATLAB Programming Language by optimizing a number of hidden layers (HLs), node numbers and training functions. The datasets are obtained from *in-vitro* NP-cell interaction experiments conducted by Nanomedicine and Advanced Technology Research Center. The dispersion characteristics and cell interactions with different NPs in organisms are explored using an optimal ANN prediction model. Simulating the possible interactions of targeted NPs with cells via an ANN model will be faster and cheaper compared to the excessive experimentation currently necessary.

Keywords: Nanomedicine, Targeted Drug Delivery, Nanoparticle Uptake Rate, Artificial Neural Networks, Prediction Model.

1. INTRODUCTION

This research aims to predict the cellular uptake rate of NPs through an appropriate ANN model using a limited number of NP-cell interaction data obtained from *in-vitro* experiments. NP-cell interaction is simulated for a 48-hour incubation period to obtain a cellular uptake rate using an optimized ANN prediction model. The proposed model can be used for NP characterization and specification of the desired cellular uptake efficiency without needing to conduct numerous experiments. Hence, the results of this research advance NPs synthesis and characterization for targeted drug delivery, diagnosis and imaging systems.

The dispersion characteristics and cell interactions of NPs in organisms are fundamental and must be investigated in targeted drug delivery research.[1] Nanoparticles with specialized agents are used especially for cell-level detection, treatment and diagnosis of existing pathologies. Research activities for treatment and diagnostic purposes have recently become more prevalent, because mortality has dramatically increased due to pathologies such as cancer. According to the World Cancer Report the burden of cancer doubled globally between 1975 and 2000, is predicted to double again by 2020 and nearly triple by 2030.[2] Current methods of diagnosis and treatment for cancer have been evolving through emerging technologies such as nanotechnology. Targeted delivery, diagnostic and imaging systems and regenerative medicine and tissue engineering are important research and development areas related to nanotechnology and biotechnology.[3]

The latest diagnostic imaging practices aim to develop NPs that can carry specific contrast material to be targeted and directed from outside the body. Current research focusing on targeted drug delivery combines NPs with pharmacological agents. NPs are characterized according to targeted tissues. Understanding NP-cell interactions is very important for targeted drug delivery and nanomedicine research. But, it is practically impossible to

*Author to whom correspondence should be addressed.

 1546-1955/2014/11/272/011 doi:10.1166/jctn.2014.3348

test all the possible combinations of NP characteristics to be able to understand and generalize the effects of nanomaterials on biological systems. Our research develops an ANN model that can simulate experimental results for any desired setup, thus eliminates time-consuming and costly experiments.

The primary contribution of our study is to the area of nanomedicine, by developing an ANN model to predict NP uptake rate. Furthermore, we simulate cellular uptakes of NPs for multiple variations of NP characterization to be able to understand NP-cell interactions without needing to conduct thousands of experiments. The second major contribution is to the field of ANN, by testing various feed-forward multilayered ANN models with different training algorithms and network structures. Specifically, this study demonstrates that an optimal ANN model is achieved using a Bayesian regularization training algorithm with a single hidden-layer structure, especially for small-sized datasets.

The remainder of the study is organized as follows: The importance and necessity of modeling the cellular uptake rate is discussed in Section 2. The relevant literature is reviewed in Section 3. The experimental procedure is laid out in Section 4 and the proposed ANN model in Section 5. The results of the computational experiments are given in Sections 6 and 7.

2. MODELING CELLULAR UPTAKE

The cellular uptake rate depends on variables such as NP size, chemical structure, shape, surface charge and NP concentration (NPs per cubic milliliter). Considering the thousands of different values of those variables, it is impossible to conduct all the necessary experiments to obtain all NP-cell interaction data within the limited scope of current NP production and experimentation. Even if it is technically feasible to produce all the required NPs, it is impractical and/or too costly to conduct all experiments in laboratory conditions. The only viable alternative is to mathematically model the complex relations between cells and NPs.

Artificial neural network models are often preferred over other mathematical models because they are more powerful for solving nonlinear complex problems. Paliwal et al. highlight the superiority of ANNs for prediction problems.[4] Out of 96 comparative studies, ANN performed better than the others in 56 cases and at least as well as the others in 23 cases.

Nonlinear NP-cell relationships must be accurately generalized by constructing and implementing a proper ANN model. Determining appropriate parameters, functions and structures of the network is essential to obtaining an optimal ANN model. We built an ANN method based on a multilayered feed-forward back-propagation algorithm to predict the cellular uptake rate of NPs, which depends on NP type, size, surface charge, concentration and time. We implemented the ANN algorithm in MATLAB Programming Language and obtained the data from *in-vitro* nanoparticle-cell interaction experiments conducted by Nanomedicine and Advanced Technology Research Center.[5]

3. LITERATURE

There are many experimental studies in the literature on the cellular uptake rate of NPs. Nanoparticles with different characteristics are experimented with to analyze the effects of NP features such as size, chemical structure, shape, surface charge and concentration. However, mathematical models of NP-cell interactions based on experimental data are rare.

Boso et al. conducted parallel-plate flow-chamber *in-vitro* experiments and used two different ANN models to predict the number of spherical NPs adhering per unit area as a function of particle diameter and wall shear rate depending on syringe pump flow rate.[6] Nateri et al. observed that ANNs technique performs better than the conventional regression method and is suitable for the simulation of the size of silver nanoparticles synthesized through Tollens process.[7] Wang et al. presented a theoretical modeling on the optical and temperature fields during gold nanoshells through combining the Monte-Carlo simulation strategy and effects of size, concentration of the nanoshells to the heating behaviors were evaluated.[8] Lin et al. performed coarse-grained molecular dynamics simulations aimed at nanoparticle's size effect on its translocation across a lipid bilayer and found that the size of NP has significant impacts on its translocation across the lipid bilayer.[9]

Rizkalla and Hildgen employed two commercial ANN models to predict mean size and micropore surface area (MPSA) of polylactic acid (PLA) nanoparticles according to polymer concentration, pressure and polyvinyl alcohol (PVA) concentration.[10] Amani et al. performed experiments to explore the effect of composition and processing factors on particle size of a nanoemulsion preparation for the delivery of fluid drugs.[11] In these studies they do not consider other properties of NPs, such as type, shape, charge and concentration.

In the last decade, NP-cell interactions have been examined to better understand the relationships between two or three variables only; the remaining NP features and environmental specifications were kept constant. Asati et al. performed experiments to determine the cellular uptake and intracellular localization of polymer-coated cerium oxide NPs with respect to surface charges.[12] Peetla and Labhasetwar used polystyrene NPs of different surface charges and sizes to analyze changes in the cell membrane's surface pressure (SP).[13] Chithrani et al. investigated the impact of different sizes and shapes of gold NPs on intracellular uptake in mammalian cells.[14] Davda and Labhasetwar observed that the cellular uptake of NPs depends on the time of incubation and that it increased

with increasing NP concentration in the medium.[15] They concluded that NP uptakes into cells show large variations with changing NP size, surface charge, concentration and measurement times. In all these studies, NP-cell interactions are examined only through physical experimentations, i.e., without any mathematical model. In this context, our study can be viewed as a first step toward mathematical modeling of NP-cell interactions.

Although nanomedicine is a new discipline, applications of ANN are common in medicine; for example, in clinical diagnosis, image analysis and interpretation, signal analysis and interpretation and drug development.[16] An artificial neural network methodology mostly enhances the quality of research. A systematic review assessed the benefit of ANNs as decision-making tools in the field of cancer. Of the 27 out of 396 studies that were clinical trials or randomized controlled trials, 21 showed an increase in benefit to healthcare provision and six did not.[17] Ahmed's review showed that applications of ANNs have improved the accuracy of colon cancer classification and survival prediction compared to other mathematical or clinicopathological methods.[18] As a result, ANN appears to be an appropriate approach for modeling complex input-output relationships in medicine.

4. EXPERIMENTAL PROCEDURE

Synthesizing NPs for targeted drug delivery and detecting existing pathologies at the cell level requires special expertise and advanced technology. Synthesized NPs should be characterized according to the targeted cell/tissue so the NPs can find and adhere to the target cell/tissue in the chaotic environment of an organism. Nanoparticles used for cell-level treatment and diagnostic purposes have five key characteristics: size, chemical structure (type), shape, surface charge and concentration.

To ensure the chemical composition, size, zeta potential, concentration and homogeneity standardization of the NPs, we obtained them from Micromod Partikeltechnologie, which produces NPs according to ISO 9001:2008 and EN ISO 13485:2003/AC2007 standards.

Considering technological constraints and scientific priorities, three types of NPs were prepared for our *in-vitro* nanoparticle-healthy cell (3T3 Swiss albino Mouse Fibroblast) interaction experiments: polymethyl methacrylate (PMMA), silica and PLA. For the PMMA and silica NPs, diameters of 50 nm and 100 nm are preferred; for the PLAs, a 250 nm diameter is preferred. Two different surface charges (positive and negative) were formed for each type of NP that are all sphere shaped. Low and high concentrations of NPs (respectively, 0.001 mg/l and 0.01 mg/l) were interacted with healthy cells.

We used transmission electron microscopy (TEM) to determine the size and size distribution of NPs inside and over the surface of the cells; surface charges were determined by zeta potential measurements. The nanoparticles were subjected to interact with cells *in vitro* using micromanipulation systems in labs. Spectrophotometric measurement methods, TEM and confocal microscopy were applied to observe NP-cell interactions and to obtain the data. Cells were incubated in a medium containing 10% FBS, 2 mm L-glutamine, 100 IU/ml penicillin and 100 mg/ml streptomycin at 37 °C with 5% CO_2. After incubation, proliferating cells in the culture flask were passaged using PBS and a trypsin-EDTA solution. Then, cells were incubated for 24 hours, counted, and placed on 96-well cell culture plates. Next, previously prepared solutions containing specific concentrations of NPs were added to those plates.

The cellular uptake rates of the NPs were measured at three, six, 12, 24, 36 and 48 hours of incubation. The experiments were repeated six times for each of 20 different configurations of nanoparticles. At the end of the incubation period, the number of NPs left in the environment was determined with washing solution.

5. PROPOSED MODEL

The proposed model is a multilayer feed-forward network, and the training process is performed with a back-propagation algorithm. The network consists of an input layer with five nodes, one hidden layer (HL) with n nodes and one output layer with one node. The values of the input variables are given in Figure 1. The output of the proposed ANN model is the cellular uptake rate of the NPs, which is the only dependent variable of the experiments. The uptake rate is the ratio of NPs on the cell surfaces or inside the cells to the total number of applied NPs.

We use the The Tan-sigmoid (tansig) transfer function for the HLs and saturated linear (satlin) transfer function for the output layer. The tansig and satlin transfer functions are given by

$$f(x) = \frac{2}{1+e^{-2x}} - 1 \quad \text{and}$$

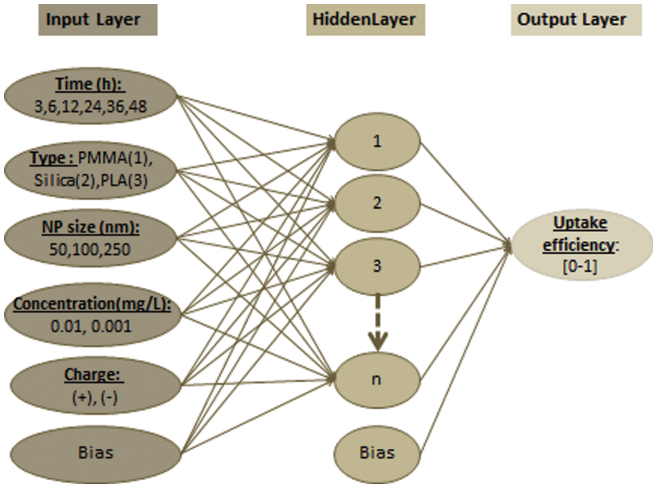

Fig. 1. ANN architecture.

$$f(x) = \begin{cases} 0 & \text{if } x < 0 \\ x, & \text{if } 0 \le x < 1 \\ 1 & x \ge 1 \end{cases}$$

respectively.[19]

The dataset is divided randomly into training and test datasets. The training dataset is used to fit the neural networks model. The test dataset is used after the training dataset to evaluate the model's performance. An unbiased estimate of the generalization error of the model is provided by the error on the test dataset. This simple validation method is known as test set validation.

Data allocation between the training and test datasets is important, because our experimental dataset is small. There are 20 different combinations of input variables, and we conducted six experiments for each combination. Increasing the class imbalance in the training dataset generally gives a gradually unfavorable result on the test performance for small- and moderate-sized training datasets.[20] One randomly selected sample is used for the test dataset, and the remaining five samples are used for training for each different combination of input variables. This method is called split-sample cross validation. In this manner, 196 samples are allocated for testing from a total of 1176 samples.

5.1. Training Parameters

Mean squared error (MSE) is used as the network performance function during the training process. The performances of 14 different training functions are measured in terms of MSE and execution time. Training function performance is tested with three different layer structures: 5-5-1, 5-10-1 and 5-15-1. The first number in each group is the input node number, the second number represents the number of nodes in the HL and the last number is the output of the network. In terms of minimum MSE over the test dataset and minimum amount of training time, the best training function is the Bayesian regularization (*trainbr*), which adjusts the weight and bias values according to the Levenberg-Marquardt optimization method.

5.2. The Number of Hidden Layers and Number of Neurons

It is argued that determining the optimal number of hidden neurons is impossible because the process depends on too many variables (e.g., numbers of input and output units, complexity of the problem, number of training iterations, amount of noise in the data, architecture of the network, training algorithm).[21] Thus, various research articles propose different rules for deciding on the optimal number of hidden neurons. The best network structure, the number of HLs and neurons are generally obtained by trial and error.

Feed-forward networks can learn complex relationships more quickly if the network has more than one HL. Haykin proposed that at most two HLs are sufficient to model every ANN problem.[22] In our study, we tested one and two HLs with different numbers of nodes that makes a total of 420 different ANN structures. The performance achieved by two HLs is comparable with one hidden layer with more than 18 neurons. We prefer a single hidden layer because computation time increases with the number of hidden layers.

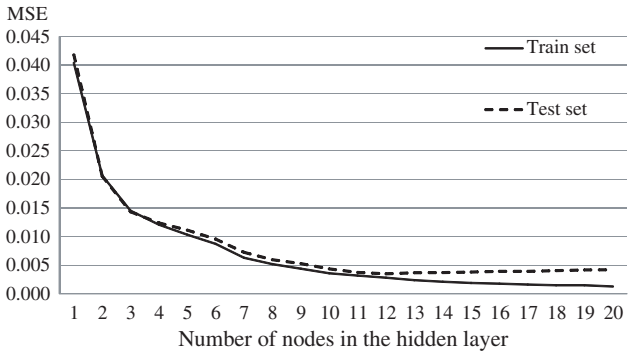

Fig. 2. The MSE of one-layer ANN models.

Figure 2 shows the MSE of the networks with different node numbers. According to these results, increasing the number of nodes sharply decreases MSE. It is seen that five nodes or fewer result in under-fitting. When more than 12 nodes are used in the hidden layer over-fitting occurs. Therefore, the best number of nodes on the hidden layer turns out to be 12.

6. SIMULATION RESULTS

The NP uptake rate is simulated for 48 hours via an optimized ANN model. The proposed ANN model has a 5-12-1 network structure and implements a Bayesian regularization training algorithm. The predicted values of the NP uptake rate are shown in 20 different charts for each combination of NP characteristics. Simulation runs were repeated 50 times for each combination and the best of 50 fits were chosen as the final mode fit. The mean uptake rates of these 50 simulated samples are plotted as black straight lines in Figures 6–10. The 95% confidence bounds, plotted as dashed lines, are calculated with $\pm 2\sigma$ (standard deviations) of the simulated 50 samples for each hour from 1 to 48. The prediction intervals are seen between upper and lower dashed lines. Data from the experiments are plotted as *o*-marks.

The prediction intervals are short at the hours when observations are made. However, prediction intervals are long at the hours when no observations are made. All observations of PLA NPs remain within the 95% confidence bounds, but too few observations are out of confidence bounds for PMMA and silica.

After adding NPs to the cell lines, cell adhesion and entry is rapidly realized in the first three hours. Although the overall behavior of NP uptake varies according to NP

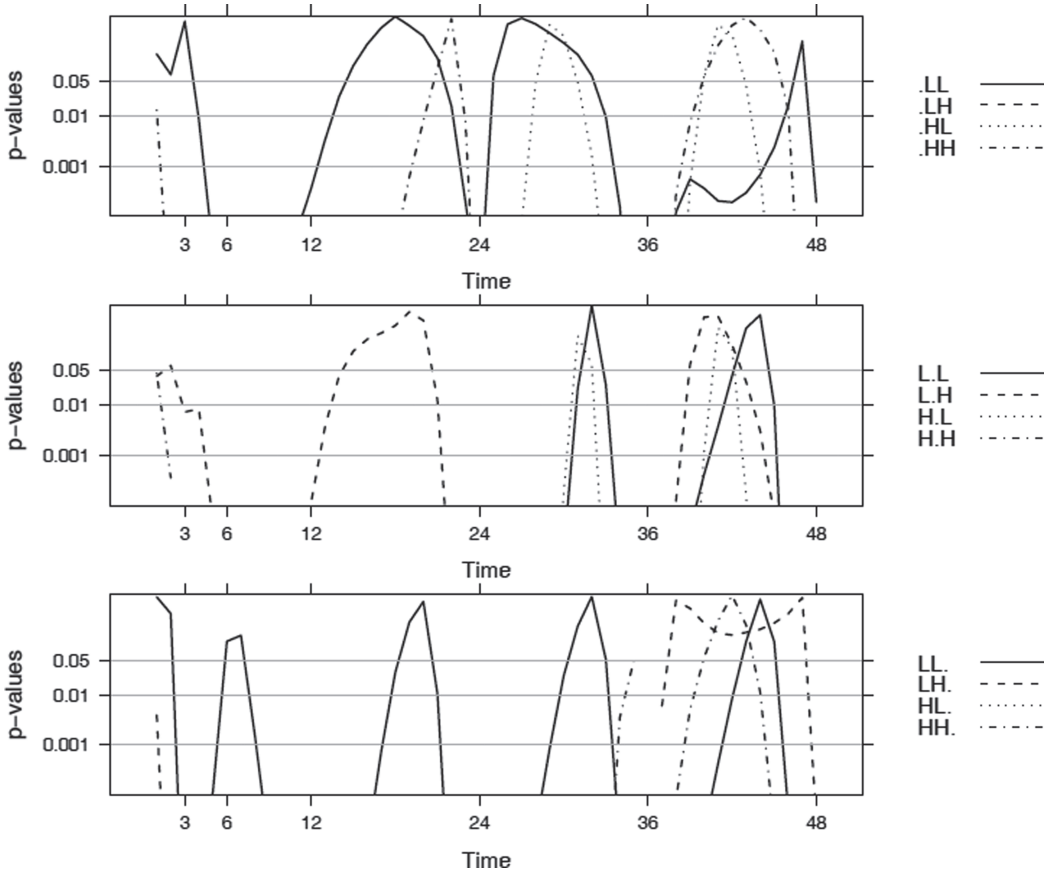

Fig. 3. *p*-values for PMMA NPs.

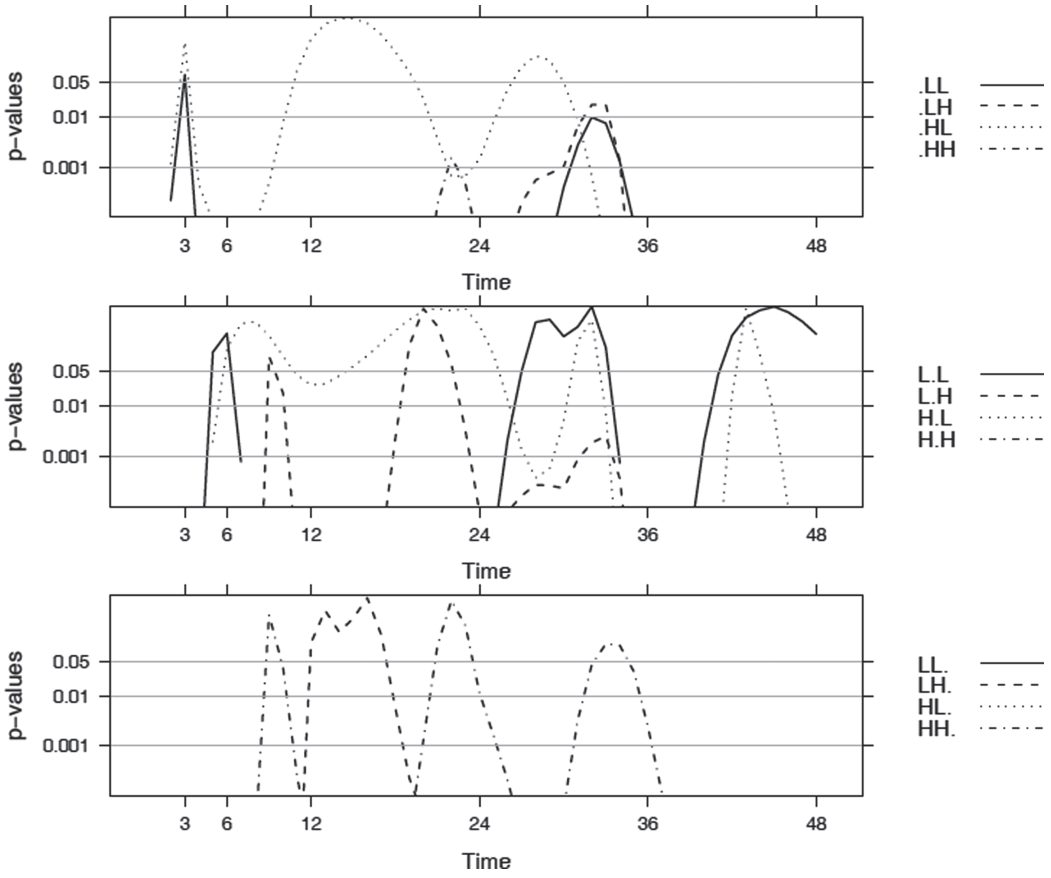

Fig. 4. *p*-values for silica NPs.

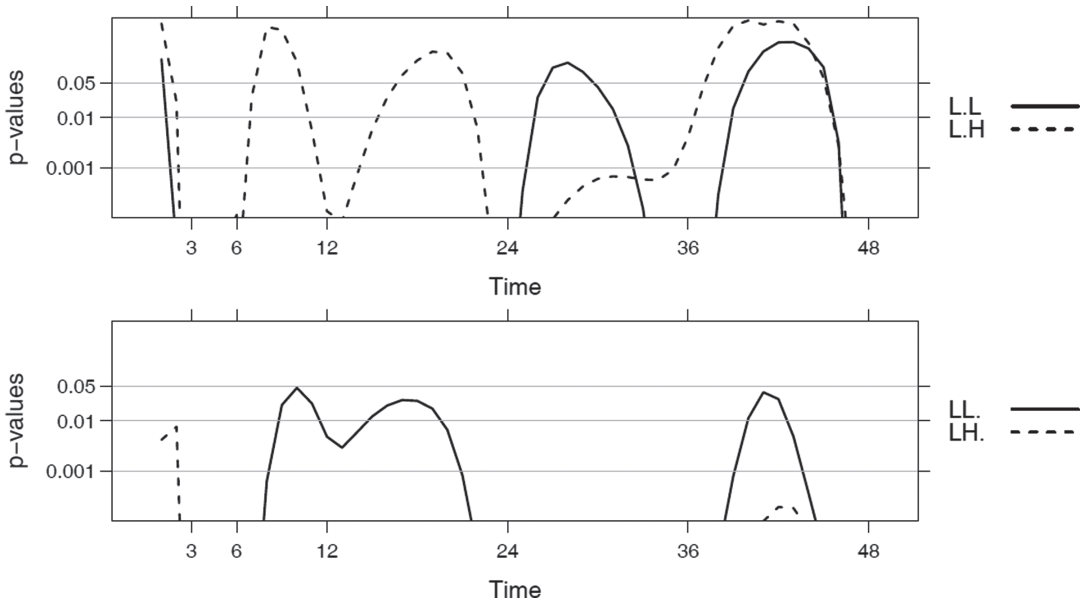

Fig. 5. *p*-values for PLA NPs.

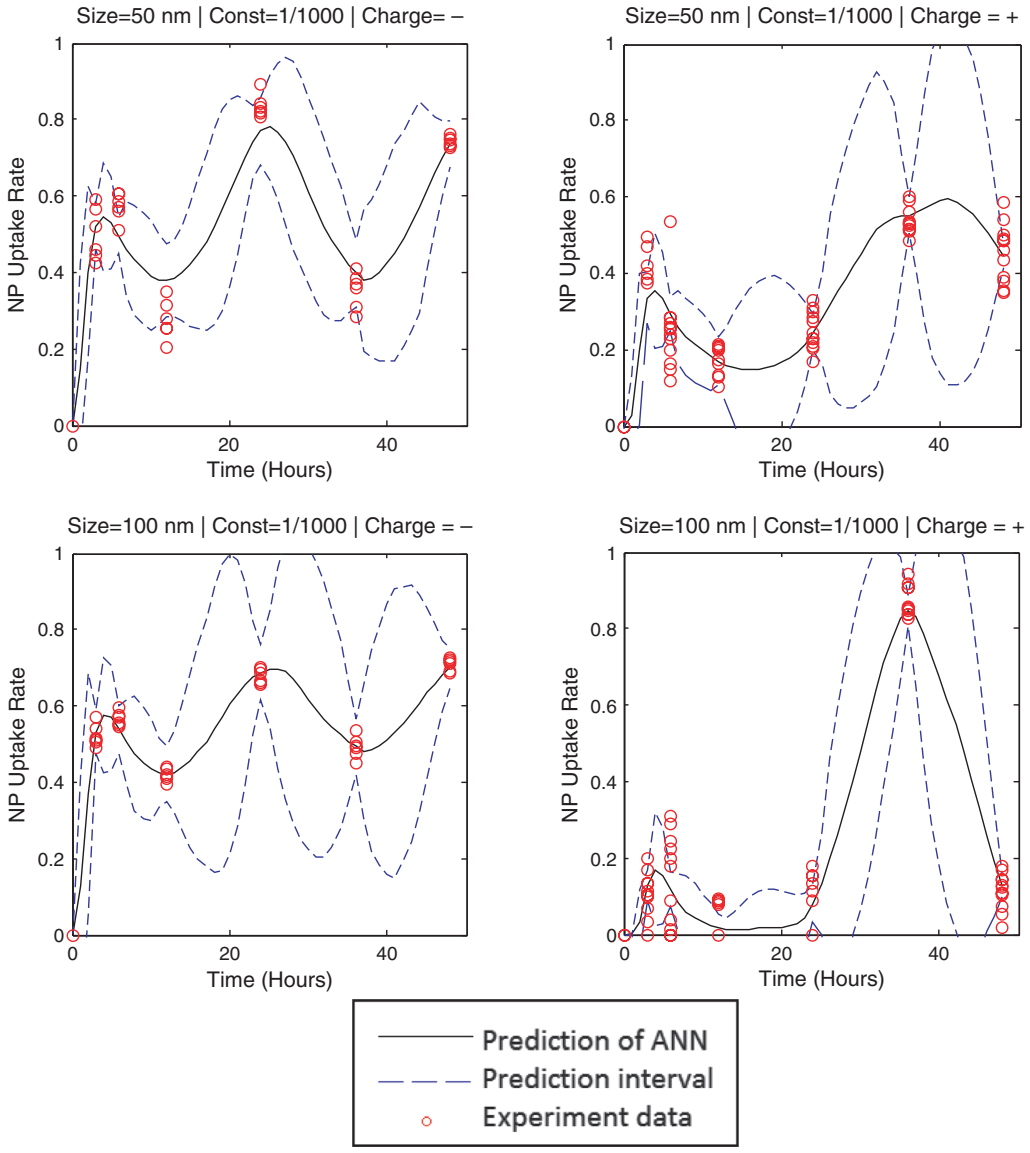

Fig. 6. PMMA simulation (Concentration: 1/1000 mg/l).

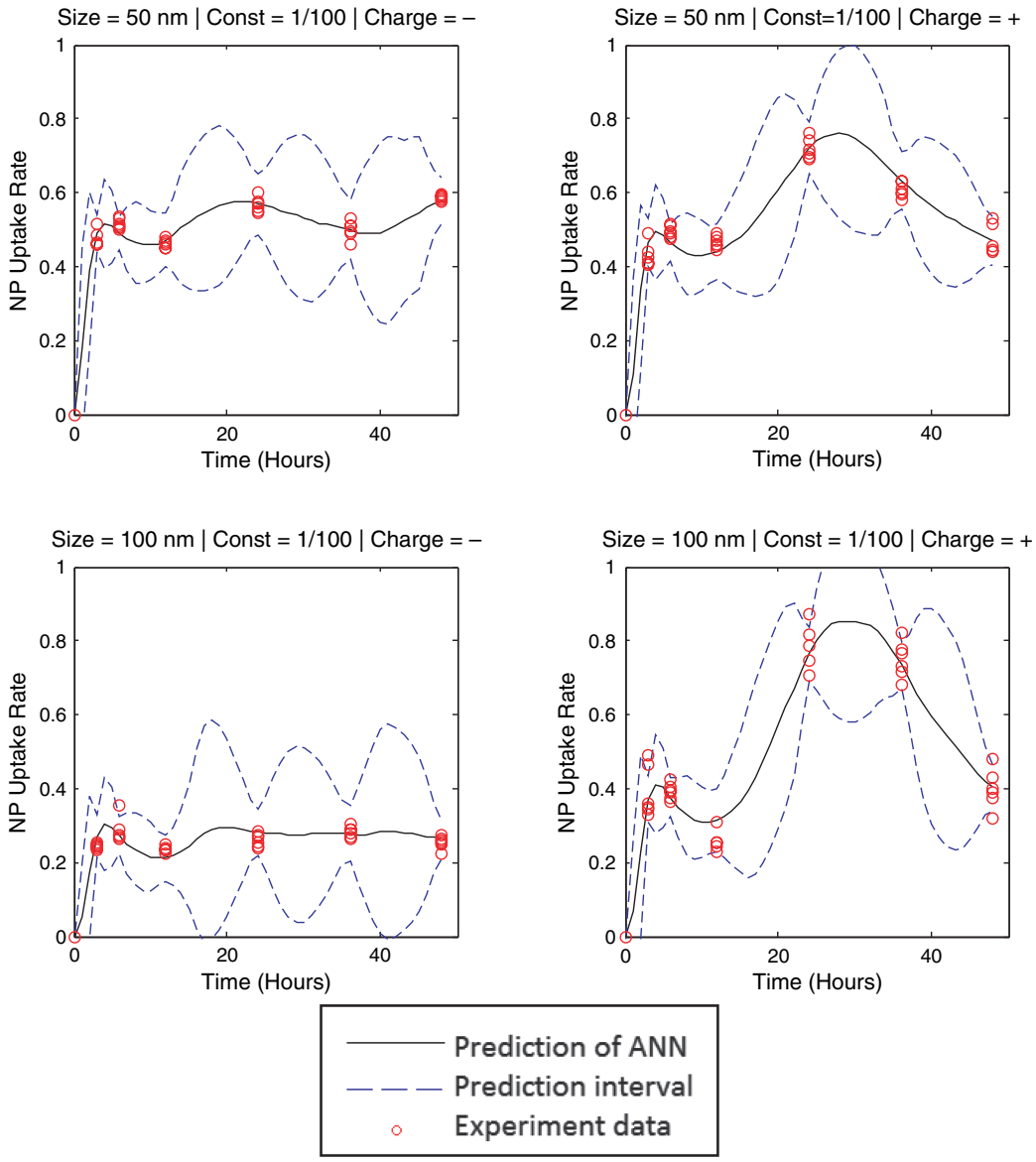

Fig. 7. PMMA simulation (Concentration: 1/100 mg/l).

characteristics, the general behaviors are similar across all the figures. At the beginning of the incubation period, there is a rapid entry of NPs into the cells. After a while, the NP uptake rate decreases, and then again increases, and continues to fluctuate in this fashion.

The mean levels and prediction intervals for the uptake rates of the PMMA nanoparticles are displayed in Figures 6 and 7. When size and concentration are constant, negatively charged NPs have short prediction intervals of hourly uptake rates. When negatively charged PMMA NPs are compared in terms of concentration with constant NP size, the high concentration (1/100) has shorter prediction intervals, which give more-stable uptake rate results than the low concentration (1/1000).

Hypothesis testing for the difference between two means is applied to understand the effect of 50 and 100 nm sizes for negatively charged PMMAs. For each hour from one to 48, we calculated mean and standard deviations of 50 samples. The central limit theorem states that the sampling distribution of a statistic will be approximately normal if the sample size is greater than 40. Thus, each sample is an independent simple random sampling with approximately normal distribution. A two-sample t-test is appropriate to determine whether the difference between means found in the sample is significantly different from the hypothesized difference between means.

Null hypothesis: effects of 50 and 100 nm sizes are the same.

Alternative hypothesis: effects of 50 and 100 nm sizes are different.

When the null hypothesis states that there is no difference between the two population means, the null and alternative hypotheses are stated as H_0: $\mu_1 = \mu_2$ and H_a: $\mu_1 \neq \mu_2$, respectively.

The significance level is 95% for this analysis. The degree of freedom (DF) is $n - 1 = 49$.

Standard error is computed as $SE = \sqrt[2]{(\sigma_1^2/n_1)+(\sigma_2^2/n_2)}$ and the t-score test statistic as $t = [(\mu_1 - \mu_2) - d]/SE$, where μ_1 is the mean of Sample 1, μ_2 is the mean of Sample 2, d is the hypothesized difference between population means ($d = 0$ for this case), σ_1 is the standard deviation of Sample 1, σ_2 is the standard deviation of Sample 2, n_1 is the size of Sample 1 and n_2 is the size of Sample 2.

The null hypothesis is rejected when the p-value is less than the significance level. Based on the two-sample t-test statistic and the DF, the p-value is determined. Since we have a two-tailed test, the p-value is the probability that a t-ratio having 49 degrees of freedom is greater than 2.01 or less than -2.01. The significance level is 0.05; $P(t < -2.01) = 0.025$ and $P(t > 2.01) = 0.025$. In order to have a p-value lower than the significance level (0.05), the t-score should be less than -2.01 or greater than 2.01. In other words, we fail to reject the null hypothesis if the t-score is between -2.01 and 2.01.

Figures 3–5 show p-values for the PMMA, silica and PLA nanoparticles, respectively. For each factor (in the order of size, charge, density), L and H stand for the low level (50 for size, $-$ for charge, 0.001 for density) and high level (100 for size, $+$ for charge, 0.01 for density) of the factor, respectively. A "·" in place of a factor means that the p-value of the t-test for the absolute difference of the mean responses for the corresponding factor is calculated, while the other factors are fixed at their respective levels. p-values are plotted on the log scale on the vertical axis.

In Figure 3, the p-value is sometimes lower than the significance level and sometimes higher or the same for $(-)$ charged low-concentration PMMA NPs. There is no clear difference between 50 nm and 100 nm sizes. In $(-)$ charged high-concentration cases, the p-values are less

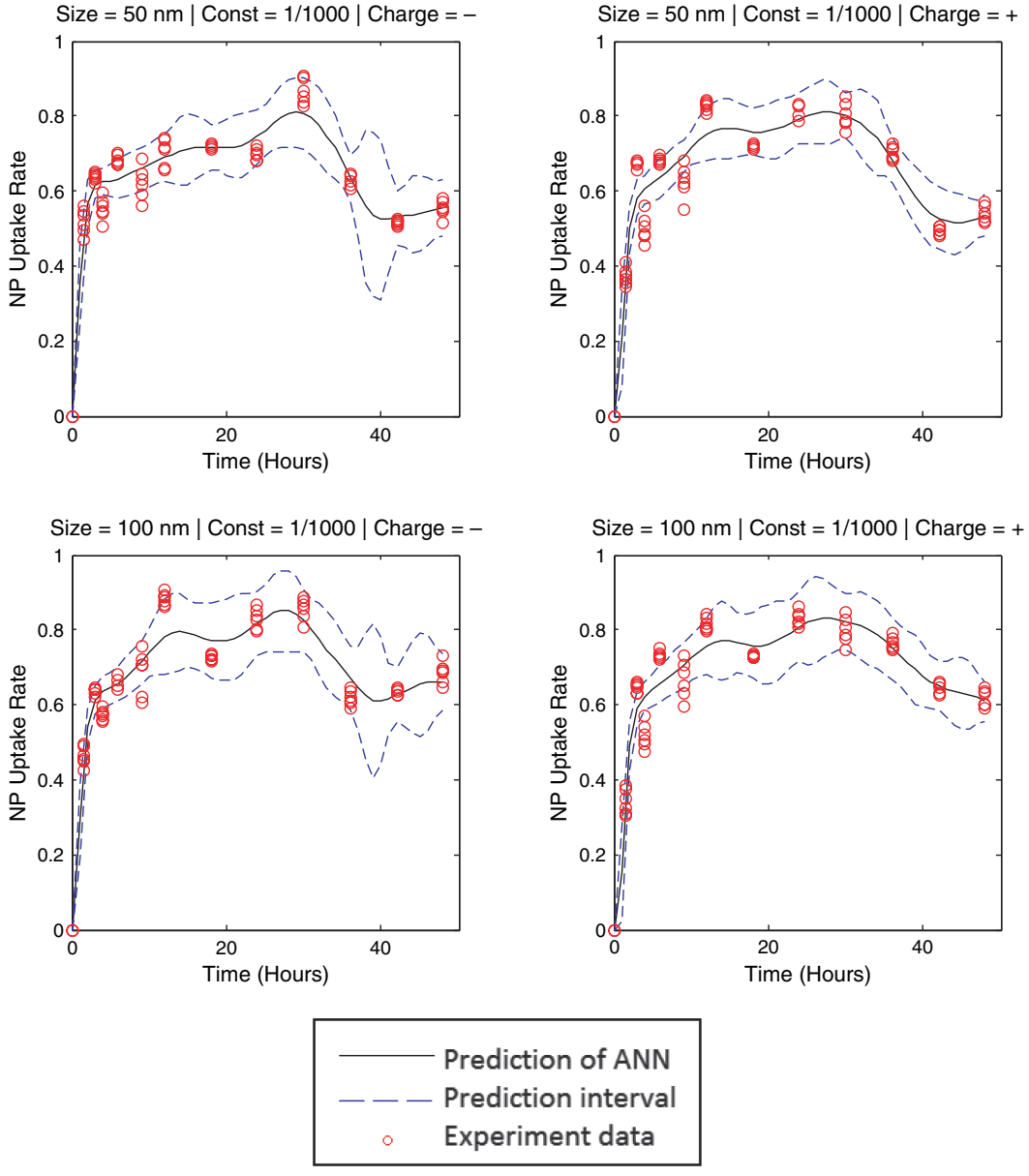

Fig. 8. Silica simulation (Concentration: 1/1000 mg/l).

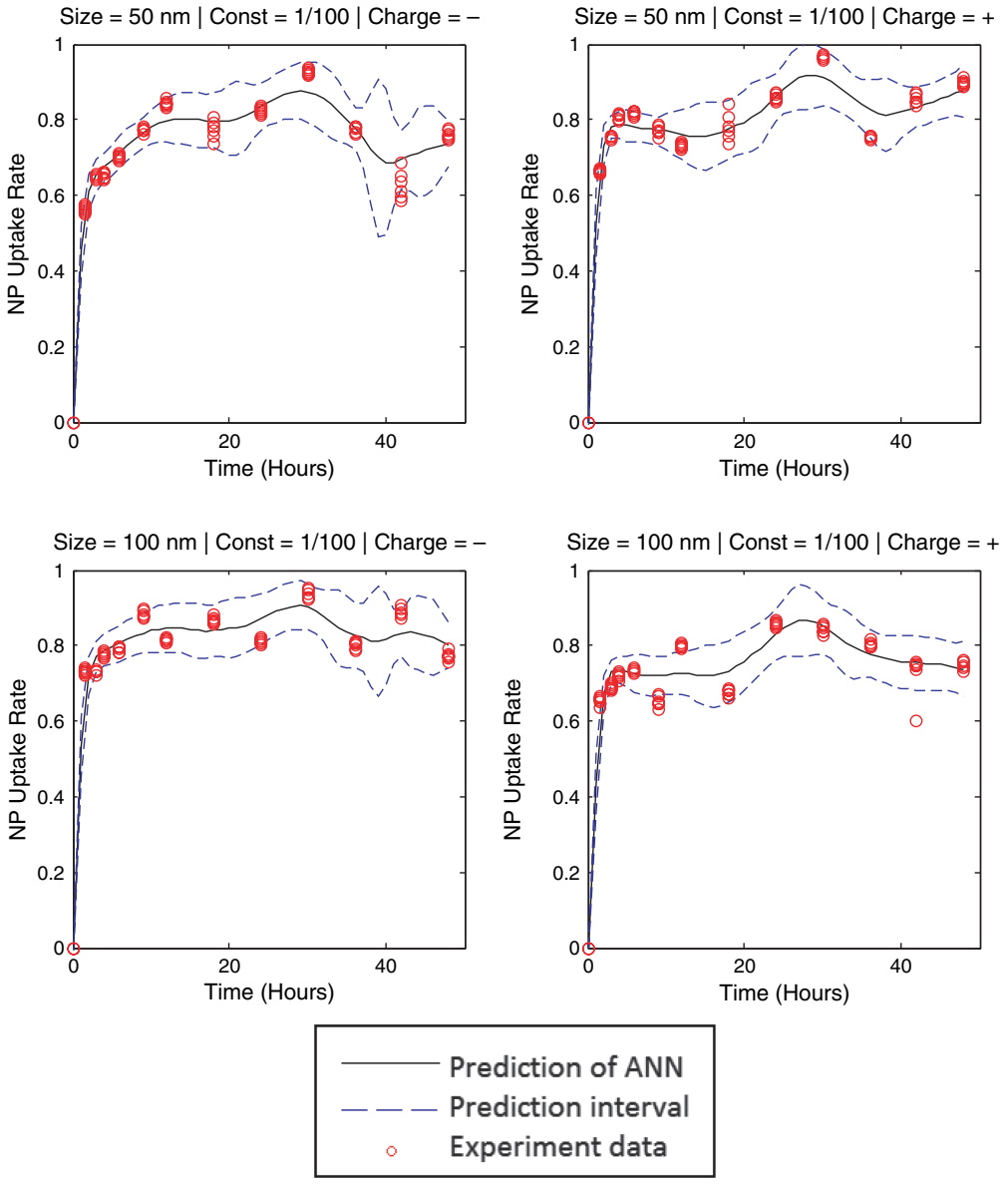

Fig. 9. Silica simulation (Concentration: 1/100 mg/l).

than 10^{-6} and t-scores are more than 2.01, hence the null hypothesis is rejected; this shows that the 50 nm size leads to a high uptake rate. According to these results, (−) charged, 50 nm and the higher-concentrated PMMA NPs are more stable and give higher uptake rate results in a targeted distribution system.

The mean levels and prediction intervals for the uptake rates of the silica NPs are given in Figures 8 and 9. We conducted the two-sample t-test (which involves the same procedure as described above for PMMA) for the difference between 50 and 100 nm sizes of silica NPs. The null hypothesis is rejected for the 0.001 and 0.01 concentrations of (−) charged NPs because the 100 nm size leads to a high uptake rate and the p-values are lower than the significance level (0.05). For (+) charged NPs of 0.01 concentration the t-scores are always more than 2.01; this means that the 50 nm size leads to a high uptake rate. However, as seen in Figure 4, there is no clear difference between the effect of 50 and 100 nm sizes for (+) charged NPs in 0.001 concentrations because the null test was rejected for some hours and failed to reject for the other hours.

Based on the standard deviation of mean uptake rates of hours for the silica NPs, the negative charge provides a slightly more stable uptake rate with shorter prediction intervals when the other variables are constant. Considering only the concentration change, the high concentration is slightly more stable and has a higher uptake rate.

It is also evident from the simulation charts that uptake rates in the high concentration (1/100) are larger than in the low concentration (1/1000) with constant NP size and NP charge. If the NP concentration is low, the uptake rate rapidly and decisively decreases soon after. One can also observe that silica shows fewer fluctuations than PMMA.

The mean levels and prediction intervals for the uptake rates of the PLA NPs of 250 nm (the only size for PLA)

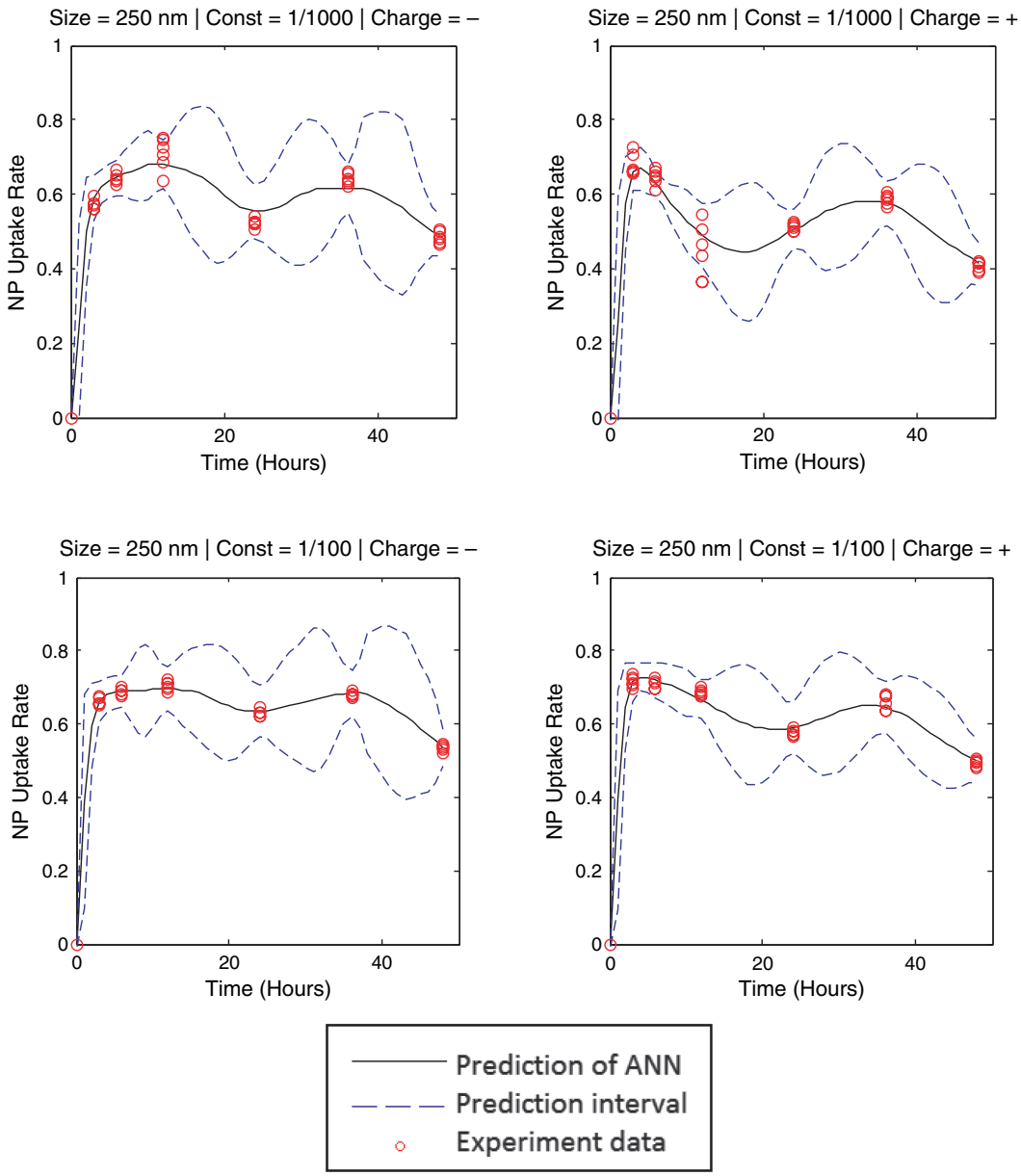

Fig. 10. PLA simulation.

are given in Figure 10. Uptake rates of PLA NPs in the high concentration (1/100) are larger than in the low concentration (1/1000). To prove this, a t-test is applied for the difference between the means of uptake rates in low and high concentrations for both charges. Results show that the t-scores are always lower than -2.01; this means that the high concentration leads to high uptake rates for $(-)$ and $(+)$ charged PLA NPs (Fig. 5).

We conducted a two-sample t-test to analyze the effect of charge difference on the PLA uptake rate. We fail to reject the null hypothesis that the negative and positive charges have equal impact. For the low concentration the null hypothesis is mostly accepted. As a result, there is no significant difference between the negative and positive charges. The $(+)$ charged PLA NPs in low concentration have the smallest standard deviation of mean uptake rates, which leads to a slightly more stable, but slow, uptake rate.

Although PLA shows fewer fluctuations than PMMA and more fluctuations than silica, there is no significant difference in the PLA nor silica results compared to the PMMA simulation results. Size and concentration impacts on uptake rate show similar results, but a marked difference between PLA and silica is realized in the surface charge. To generalize these results more accurately, it would be necessary to repeat the experiments with a wide range of NP sizes and concentrations.

7. CONCLUSION

We investigate nanoparticle-cell interactions for targeted drug delivery systems in the treatment of many diseases, including cancer. The main objective of this treatment method is to develop nanoparticle structures such that they go directly to the targeted cells, release the therapeutic

agent and are discarded from the body with no toxic effects. In this manner, highly efficient treatment can be provided with fewer drug doses and systemic side effects.

Many factors affect the rate of NPs adhering to the cell surface and entering the cell, such as concentration of NPs, surface charge, chemical structure, shape and size. To determine the ideal structure for nanoparticle characterization, NP-cell interactions must be understood. All possible NP variations cannot be tested experimentally, so devising a mathematical model for this purpose was essential. Such a modeling study is currently not present in the literature; hence our contribution.

This study develops an ANN model to predict cellular NP uptake rate. We tested several feed-forward multilayered ANN models with 14 different back-propagation training algorithms and network structures with up to two hidden layers and 20 hidden nodes. Our proposed ANN model uses the Bayesian regularization training algorithm with a single hidden layer and 12 hidden nodes.

To understand NP-cell interaction, we simulated our ANN model for 48 hours to estimate the uptake of different NP classifications. Uptake rates change mainly depending on the type of NP. Silica NPs show fewer fluctuations in uptake rate than PMMA and PLA NPs. Negatively charged NPs have more stable uptake rates than positively charged NPs. A negative surface charge especially produces more stable the uptake rate of PMMA nanoparticles. Uptake rates of PLA and silica NPs are higher in a high concentration (1/100) than in a low concentration (1/1000). There are no general findings for the effect on uptake rate of 50 or 100 nm NPs.

In future work, prediction of NP uptake rate could be modeled by other statistical methods, such as multi-linear regression models, additive mix models or support vector machines. Moreover, the results of other statistical models should be compared and combined with the current study. We tested our proposed ANN model with only *in-vitro* experiment data. *In-vivo* tissue experiments should be conducted at the level of tissues and organs. In addition, similar experiments should be repeated in different pathological cells and modeled with ANN and/or other statistical tools.

References

1. Asati A H. Elhaes, O. Osman, and M. Ibrahim, *J. Comput. Theor. Nanosci.* 9, 901 **(2012)**.
2. P. Boyle and B. Levin, World Cancer Report, International Agency for Research on Cancer, Lyon **(2008)**.
3. Y. Zhang, M. Yang, N. G. Portney, D. Cui, G. Budak, E. Ozbay, M. Ozkan, and C. S. Ozkan, *J. Biomedical Microdevices* 10, 2 **(2008)**.
4. M. Paliwal, U. A. Kumar, *Expert Systems with Applications* 36, 2 **(2009)**.
5. MATLAB, The Language of Technical Computing **(2011)**.
6. D. P. Boso, S. Lee, M. Ferrari, B. A. Schrefler, and P. Decuzzi, *Int. J. Nanomedicine* 1517 **(2011)**.
7. A. S. Nateri, S. Dadvar, A. Oroumei, and E. Ekrami, *J. Comput. Theor. Nanosci.* 8, 713 **(2011)**.
8. X. Wang, X. Gao, and J. Liu, *J. Comput. Theor. Nanosci.* 7, 1025 **(2010)**.
9. X. Lin, Y. Li, and N. Gu, *J. Comput. Theor. Nanosci.* 7, 269 **(2010)**.
10. N. Rizkalla, and P. Hildgen, *Drug Dev. Ind. Pharm.* 31, 1019 **(2005)**.
11. A. Amani, P. York, H. Chrystyn, B. J. Clark, and Q. D. Duong, *European Journal of Pharmaceutical Sciences* 35, 42 **(2008)**.
12. A. Asati, S. Santra, C. Kaittanis, and J. M. Perez, *ACS Nano* 5321 **(2010)**.
13. C. Peetla and V. Labhasetwar, *Molecular Pharmaceutics* 5, 418 **(2008)**.
14. B. D. Chithrani, A. A. Ghazani, and W. C. W. Chan, *Nano Letters* 6, 662 **(2006)**.
15. J. Davda and V. Labhasetwar, *Int. J. Pharm.* 233, 51 **(2001)**.
16. R. Thomson and M. Sordo, Open Clinical: Knowledge Management for Medical Care, Introduction to Neural Networks in Healthcare, Harvard **(2002)**.
17. P. J. Lisboa and A. F. G. Taktak, *Neural Networks* 19, 408 **(2006)**.
18. F. E. Ahmed, *Molecular Cancer* 4, 29 **(2005)**.
19. M. H. Beale, M. T. Hagan, and H. B. Demuth, Neural Network Toolbox-User's Guide, The Math Works Inc., Natick, MA **(2011)**.
20. M. A. Mazurowski, P. A. Habas, J. M. Zurada, J. Y. Lo, J. A. Baker, and G. D. Tourassi, *Neural Networks* 2, 427 **(2007)**.
21. S. Xu and L. Chen, A novel approach for determining the optimal number of hidden layer neurons for FNN's and its application in data mining, *Proceedings of 5th International Conference on Information, Technology and Applications*, ICITA, Macquarie Scientific Publishing, Bathurst, N.S.W. **(2008)**, pp. 683–686.
22. S. Haykin, Neural Networks: A Comprehensive Foundation, 2nd edn., Prentice-Hall, Upper Saddle River, NJ, USA **(1999)**.

Received: 23 October 2012. Accepted: 23 November 2012.